JOURNAL OF MATERIALS SCIENCE 24 (1989) 1700–1706

Does fabric tensor exist for a fabric?

AYDIN TÖZEREN
Department of Mechanical Engineering, The Catholic University of America, Washington, D.C. 20064, USA
RICHARD SKALAK
Department of Civil Engineering and Engineering Mechanics, Columbia University, New York 10027, USA

It is shown that the mean intercept length distribution for planar fibre networks or for materials composed of a set of plates is not in general elliptic and cannot be expressed analytically in terms of a second-order tensor. However, our numerical computations indicate that the polar plot of the mean intercept length at the angle of measurement may become nearly ellipsoidal as the microstructure (fibres or plates) become less discretely organized, but yet remain orthotropic. The equations presented in this study may be used to obtain fibre (plate) orientation density functions from the experimental data on mean intercept length distribution.

1. Introduction

The purpose of the present study is to formulate mathematically the correspondence between mean intercept length distribution and fibre orientation density in a plane fibre network. The mathematical analysis developed here is equally valid for a three-dimensional material that is composed of sets of parallel plates. Mean intercept length (L) is defined as the average distance between the interfaces of a microstructure measured along a straight line. Experimental data on cancellous bone samples showed that the polar plot of L at the angle of measurement generates an ellipse in any plane cross-section intersecting a bone sample [1, 2]. Harrigan and Mann [2] showed that, under these conditions, L could be expressed in terms of a second-order tensor called the mean intercept length tensor. More recently, Cowin [3, 4] has postulated a constitutive relation between stress in a biological tissue that has microstructure (bone, skin) and fabric tensor that also depends only on the mean intercept length distribution. Because the existence of the aforementioned microstructural tensors depend on whether the resulting mean intercept length distribution can be adequately described by an ellipsoid, we have considered this condition analytically for composites made of plates or fibres. In Section 2, we present mathematical expressions relating mean intercept length density to the fibre (plate) orientation density. We show that fabric tensor does not exist for fibre networks with a discrete number of distinct fibre directions. The results and their implications on the study of remodelling of soft biological tissues are discussed in the last section.

2. Derivations

In this section we derive a closed form expression for the mean intercept length distribution of a material composed of sets of parallel plates and show that this distribution cannot be described mathematically in terms of a second-order symmetric tensor.

Let us consider a composite material made up of sets of parallel plates embedded in an isotropic matrix (Fig. 1). The plates in different sets are assumed to coexist at the region of intersection. Any planar cross-section of the composite will then look like a fabric composed of sets of two-dimensional parallel fibres with thickness equal to the oblique thickness of the corresponding plates. Let a_i, $i = 1, 2, 3$, be a unit vector along which the mean intercept length L is measured ($L = L(a_i)$). A set of parallel plates in the composite (α) is identified by the common unit normal $\boldsymbol{n}^{(\alpha)}$, $\alpha = 1, 2, \ldots, N$. The parameter N denotes the number of plates with distinct orientations that exist in the composite. The directional sense of the unit vector $n_i^{(\alpha)}$ is chosen such that the dot product of $n_i^{(\alpha)}$ with a_i is greater than or equal to zero ($n_i^{(\alpha)} a_i \geq 0$). Summation is implied when an index is repeated twice in a term of a mathematical expression.

The mean intercept length for the composite can be obtained by summing the reciprocals of the mean intercept length $1/L^{(\alpha)}$ computed for each set of plates independently, i.e.

$$\frac{1}{L} = \sum_{\alpha=1}^{N} \frac{1}{L^{(\alpha)}} \qquad (1)$$

where $\Sigma_{\alpha=1}^{N}$ denotes summation over the sets of plates with distinct orientations. From geometric relations and noting that the number of intersections increase by two each time the line on which L is measured crosses a plate, it can be shown that L satisfies the following expression (Fig. 1)

$$\frac{1}{L} = \sum_{\alpha=1}^{N} \frac{2}{b^{(\alpha)}} a_i n_i^{(\alpha)} \qquad (2)$$

where $(1/b^{(\alpha)})$ is the number of plates per unit length in direction $\boldsymbol{n}^{(\alpha)}$, i.e. $b^{(\alpha)}$ is the spacing of the plate set α. Equations 1 and 2 hold for infinitely thin plates so there is essentially zero common volume. For thick plates, there will be mutual interference and the equations will be more complicated. Harrigan and

0022–2461/89 $03.00 + .12

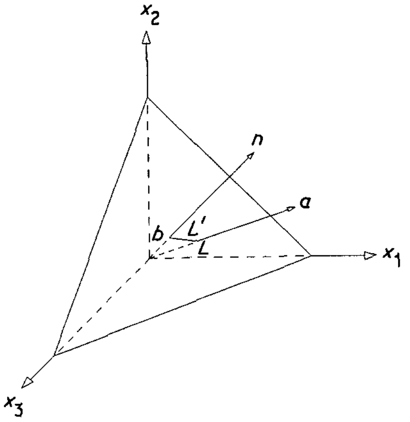

Figure 1 Three-dimensional plate network made up of sets of parallel plates. Only one plate is shown. The neighbouring plate passes through the origin.

Mann [2] previously showed that if L, plotted as a radius at the angle of measurement, generates a surface of an ellipsoid, then $1/L^2$ can be represented as

$$\frac{1}{L^2} = M_{ij}a_ia_j \tag{3}$$

where M_{ij} is defined as material anisotropy (mean intercept length) tensor. It is a second-order symmetric tensor whose components are determined from the equation of the ellipsoid generated by the mean intercept length distribution.

Using Equation 2, it can be shown that $(1/L^2)$ for the simple composite considered in the present treatment also satisfies the quadratic Equation 3, but the resulting symmetric matrix M_{ij} is not a tensor. Matrix M_{ij} in this case can be shown to be equal to

$$M_{ij} = 2\sum_{\alpha=1}^{N}\sum_{\beta=1}^{N}\left(\frac{1}{b^{(\alpha)}}\right)\left(\frac{1}{b^{(\beta)}}\right)(n_i^{(\alpha)}n_j^{(\beta)} + n_j^{(\alpha)}n_i^{(\beta)}) \tag{4}$$

A necessary condition for M_{ij} to be a second-order tensor is that M_{ij} should be independent of the direction a_i along which L is measured. But, in the derivation of Equation 2, we have assumed that the sense of $n_i^{(\alpha)}$ is chosen such that the scalar product of $n_i^{(\alpha)}$ with a_i would be greater or equal to zero. Hence, M_{ij} is not independent of a_i. This point can be illustrated by considering a composite material with two sets of plates normal to x_1 and x_2 directions, respectively.

Using Equation 4, it can be shown that

$$M_{11} = 4\left(\frac{1}{b^{(1)}}\right)^2$$

$$M_{22} = 4\left(\frac{1}{b^{(2)}}\right)^2$$

$$M_{33} = M_{13} = M_{23} = 0$$

$$M_{12} = 4\left(\frac{1}{b^{(1)}}\right)\left(\frac{1}{b^{(2)}}\right)\Gamma = M_{21} \tag{5}$$

where $\Gamma = +1$ if $(a_i > 0, a_2 > 0)$ or $(a_1 < 0, a_2 < 0)$ and $\Gamma = -1$ if $(a_1 < 0, a_2 > 0)$ or $(a_1 > 0, a_2 < 0)$. Because M_{ij} is not independent of a_i, it is not a tensor in this case. The polar plot of L in the x, y plane at the angle of measurement θ (so $a_1 = \cos\theta$, $a_2 = \sin\theta$) is not an ellipse, but is composed of four straight line segments (Fig. 2).

The fact that the plot of L against θ is a straight line in each quadrant, but $1/L^2$ has the form of Equation 3, can be reconciled by considering L as a function of θ for any straight line in the x, y plane not passing through the origin. Here L is the distance from the origin to the line. It can be readily shown that for the line

$$y = b - mx \quad (b > 0, m > 0) \tag{6}$$

that

$$M_{ij} = \frac{1}{b^2}\begin{bmatrix} m^2 & m \\ m & 1 \end{bmatrix} \tag{7}$$

Thus, Equation 3 may describe a straight line $L(\theta)$, but when it does, $|M| = 0$. The alternation of Γ in Equation 5 gives the four different straight lines in Fig. 2c.

If more sets of plates perpendicular to the x_1, x_2 plane are added, as in Fig. 2b, then similar expressions can be derived, with a change of sign of a Γ factor each time the normal $n^{(\alpha)}$ of set (α) becomes perpendicular to the θ direction. In between such changes, $1/L^2$ has the form of Equation 3, but $|M_{ij}| = 0$ so the plot of $L(\theta)$ is a sequence of straight lines.

In the general three-dimensional case, for a discrete number, N, of sets of planes, there will be solid angles (bounded by planes) within which M_{ij} in Equation 3 are constant. But it can be shown that $|M_{ij}| = 0$ and that it follows that $L(a_i)$ within these regions lies on a plane, not intersecting the origin. Thus, the three-dimensional surface $L(a_i)$ is a polyhedral closed surface for a discrete number, N, of sets of planes. It is not an ellipsoid and $|M_{ij}| = 0$ on each face. (See Appendix for proofs.)

The analysis described above is equally valid for a plane fibre network provided that the spacial indices in Equations 2 and 4 are restricted to the values $i = 1$ and 2. Therefore, the mean intercept length distribution matrix, M_{ij}, is not a second-order tensor for a fabric (plane fibre network) with a discrete number, N, of sets of fibres.

Recently, Cowin defined a tensor $\boldsymbol{H}$ called fabric tensor as:

$$\boldsymbol{H} = \boldsymbol{M}^{-1/2} \tag{8}$$

where M_{ij} is the symmetric tensor defined by Equation 3. Because M_{ij} may not be a positive definite tensor for a fabric as illustrated with the example given above, the applicability of a fabric tensor for a plane fibre network (fabric) is not established. Our numerical

TABLE I Mean intercept length distribution (L) corresponding to the fibre orientation density $Q = |\cos\phi|/2$

Direction, θ (deg)	Mean intercept length L (Eq. 8)	L evaluated by tensorial expression (Eqs 3, 12)
0	1	1
30	0.886	0.855
45	0.795	0.763
60	0.711	0.689
90	0.637	0.637

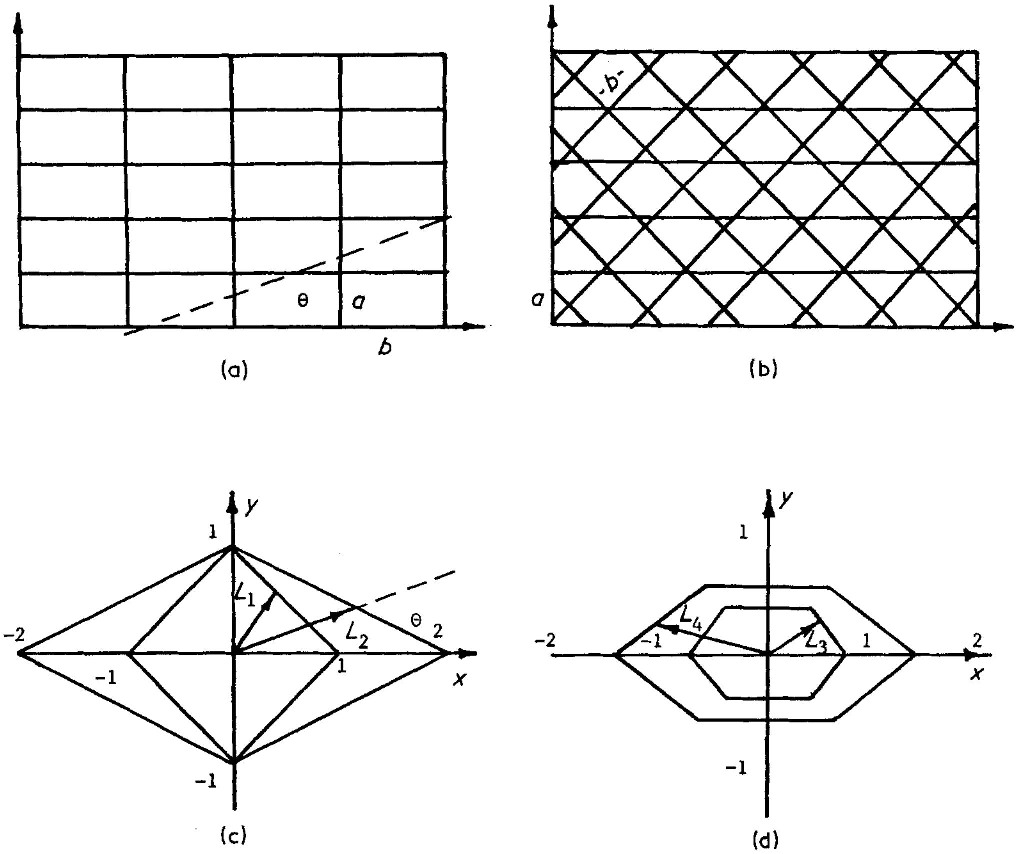

NETWORK	DIMENSIONS	MEAN INTERCEPT LENGTH
1	$b = a = 1$ in (a)	L_1 in (c)
2	$b = 2,\ a = 1$ in (a)	L_2 in (c)
3	$b = a = 1$ in (b)	L_3 in (d)
4	$b = 2,\ a = 1$ in (b)	L_4 in (d)

Figure 2 Four distinct fibre networks and the corresponding mean intercept length distributions. The parameters of the four networks are shown in the table inset. The topology of networks 1 and 2 are shown in (a) and that of networks 3 and 4 in (b). The dimensions a and b define the distances between axes of adjacent parallel fibres. The mean intercept lengths L_3 and L_4 for networks 3 and 4 are shown in (d). In each case, the mean intercept length $L(\theta)$ is indicated by the radial distance to the curve shown at each θ. Each curve is plotted in the same x, y plane in (c) and (d) as in (a) and (b) to indicate the orientation θ with respect to the same x, y axes.

computations indicate that the deviation of the mean intercept length distribution from that of an ellipsoid tends to decrease as the number of distinct fibre (plate) directions increases. For this reason we have next considered a plane fibre network with a continuous distribution of fibre orientations. The mean intercept length L satisfies the following integral equation in this case:

$$\frac{1}{L(\theta)} = 2\int_0^{\pi} Q(\phi)\sin(|\theta - \phi|)\,d\phi \qquad (9)$$

where θ is the angle at which L is measured (so $a_1 = \cos\theta$, $a_2 = \sin\theta$) and $Q(\phi)$ is the number density per unit length of fibres with orientation $\boldsymbol{e}$ (i.e.) $e_1 = \cos\phi$, $e_2 = \sin\phi$).

Let us consider the simple case of $Q(\phi) = Q_0|\cos\phi|$ for which a closed form integration of Equation 9 is possible. The parameter $(1/L)$ can then be shown to satisfy the following equation

$$\frac{1}{L} = 2Q_0(\cos\theta + \theta\sin\theta)\left(0 < \theta < \frac{\pi}{2}\right) \qquad (10)$$

The components of M_{ij} corresponding to Equation 10 can be written as

$$M_{11} = 4Q_0^2 \qquad M_{22} = 4Q_0^2\theta^2$$

$$M_{12} = 8Q_0^2\theta \qquad -\frac{\pi}{2} \leqslant \theta \leqslant \frac{\pi}{2} \qquad (11)$$

Hence, M_{ij} clearly depends on θ; therefore, it is not a tensor. However, the polar plot of $L = L(\theta)$ is nearly elliptic for $Q = Q_0|\cos\phi|$ (Fig. 3). The major and minor radii of the elliptical approximation to the L distribution are $1/2Q_0$ along x_1 axis and $(1/\pi Q_0)$ along x_2 axis. M_{ij} corresponding to this ellipse can be shown to be equal to

$$M_{11} = 4Q_0^2 \qquad M_{22} = \pi^2 Q_0^2 \qquad M_{12} = 0 \qquad (12)$$

This example provides an analytical illustration consistent with the observation that mean intercept length distribution becomes nearly elliptic as the fibre network becomes less discretely organized, preserves orthotropic symmetry but is not, in fact, representable by a constant tensor M_{ij} in Equation 3. In such cases mean intercept length tensor can be constructed as shown by Harrigan and Mann [2] by curve fitting

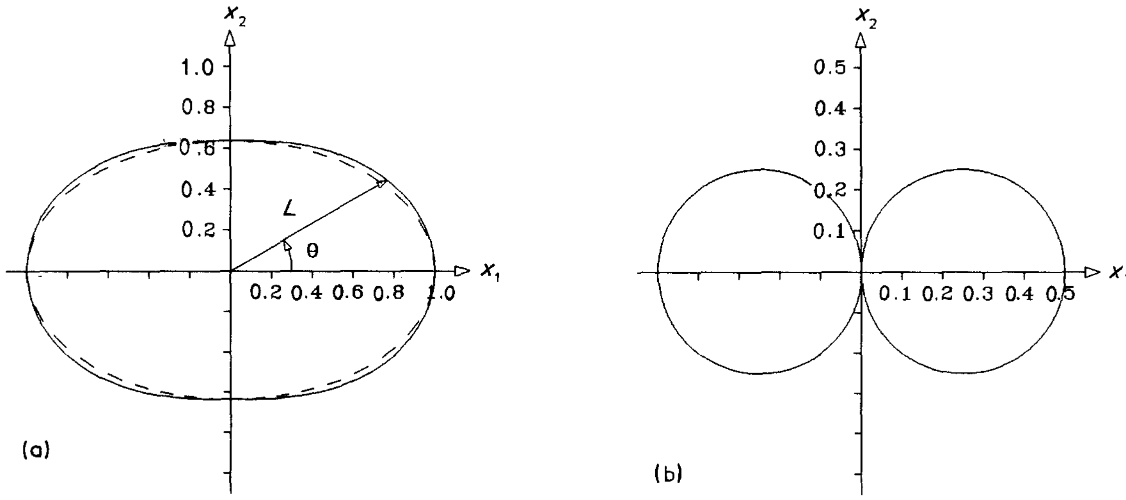

Figure 3 Mean intercept length distribution L(a) corresponding to the fibre orientation density $Q = (1/2)|\cos\theta|$ (b). The continuous lines in (a) represent the actual mean intercept length distribution. The curve shown with discrete lines represents the ellipsoidal approximation.

the polar plot of L with the equation of an ellipsoid so that M_{ij} becomes a constant tensor and represents the data reasonably well. Not all continuous fibre distributions yield polar plots of L that are very nearly elliptic. Consider, for example, the case of $Q = Q_0|\sin 2\theta|$. It can be shown that the mean intercept length L in this case can be expressed in terms of θ as

$$\frac{1}{L} = \tfrac{8}{3}\, Q_0(\sin\theta + \cos\theta - \sin\theta\cos\theta)$$

$$0 \leqslant \theta \leqslant \frac{\pi}{2} \tag{13}$$

The polar plot of L as a function of θ, as shown in Fig. 4, is not an ellipse.

There probably are distributions $Q(a_i)$ of planes in three dimensions or $Q(\phi)$ in two dimensions which give distributions of $L(a_i)$ or $L(\theta)$ which are ellipsoidal or plane ellipses, but such distributions are not known in closed form at present.

3. Elastic coefficient tensor of a fabric and the fabric tensor

In the previous section it has been shown that the mean intercept length distribution can be represented with reasonable accuracy for some fabrics with continuous fibre orientation density by an approximate elliptical mean intercept length and that H_{ij} exists, approximately. In this section we investigate the relation between fabric tensor H_{ij} and the elastic coefficient tensor of a fabric.

The stress–strain relation of a plane fibre network with elastic fibres is linear in the presence of small deformations

$$\sigma_{ij} = C^{*}_{ijkl} e_{kl} \tag{14}$$

where σ_{ij} and e_{kl} are the stress and strain tensors and C^{*}_{ijkl} is the elasticity coefficient tensor. The elasticity coefficient tensor will have contributions from the fibres as well as the matrix in which the fibres are embedded. For simplicity we shall consider below only the part of C^{*}_{ijkl} that is contributed by the fibres in the matrix (C_{ijkl}). It can be shown that [5]

$$C_{ijkl} = 2D \int_{-\pi/2}^{\pi/2} P(\theta) b_i b_j b_k b_l \, \mathrm{d}\theta \tag{15}$$

where the unit vector $\boldsymbol{b}$ denotes the fibre direction, $P = P(\theta)$, is the fibre density distribution, and D is a material constant which is a measure of fibre stiffness. In the case of a fibre network with uniform fibre

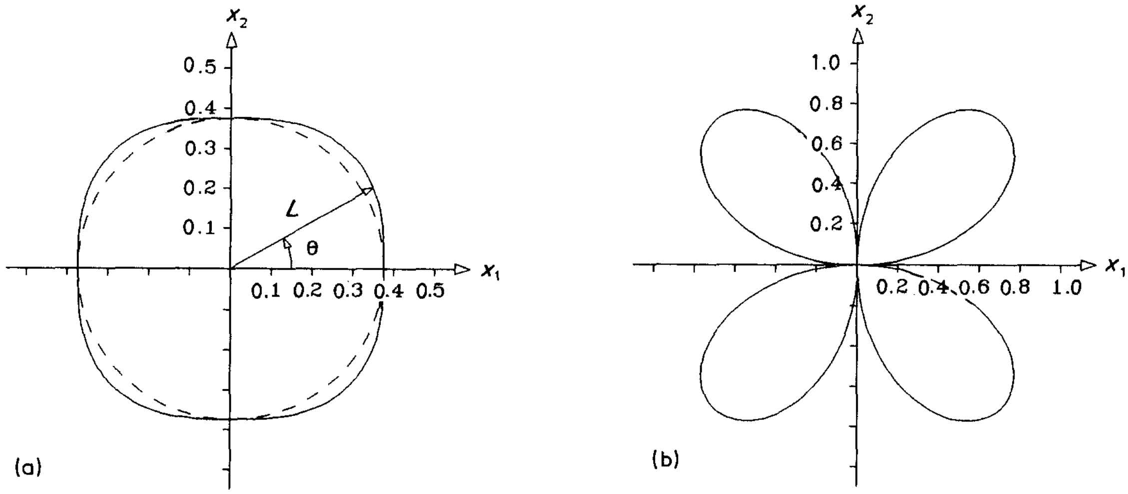

Figure 4 Mean intercept length distribution L(a) corresponding to the fibre orientation density $Q = \sin|2\theta|$ (b). The continuous lines in (a) represent the actual mean intercept length distribution. The curve shown with discrete lines represents the ellipsoidal approximation.

diameter d, P is related to the fibre number density Q by the equation $P = Q(\pi d^2/4)$. The components of C_{ijkl} can easily be evaluated once the fibre density distribution is known. For example, for the fabric with $Q = Q_0|\cos\theta|$ considered in the previous section, it can be shown by substituting $P(\theta)$ in Equation 15 that

$$C_{1111} = (16/15)\frac{\pi d^2}{4}Q_0 D$$

$$C_{2222} = (6/15)\frac{\pi d^2}{4}Q_0 D$$

$$C_{1122} = C_{2211} = C_{1212} = C_{2112} = C_{1221} = C_{2121} = \frac{\pi d^2}{15}Q_0 D \qquad (16)$$

and all other components are equal to zero.

Recently, Cowin [6] proposed the following constitutive relation for a porous elastic solid in which the anisotropic behaviour is due only to the geometry of the microstructure represented by the fabric tensor $\boldsymbol{H}$

$$\begin{aligned} C_{ijkm} = {} & a_1\delta_{ij}\delta_{km} + a_2(H_{ij}\delta_{km} + \delta_{ij}H_{km}) \\ & + a_3(\delta_{ij}H_{kq}H_{qm} + \delta_{km}H_{iq}H_{qj}) + b_1H_{ij}H_{km} \\ & + b_2(H_{ij}H_{kq}H_{qm} + H_{is}H_{sj}H_{km}) \\ & + b_3H_{is}H_{sj}H_{kq}H_{qm} + c_1(\delta_{ki}\delta_{mj} + \delta_{mi}\delta_{kj}) \\ & + c_2(H_{ik}\delta_{mj} + H_{kj}\delta_{mi} + H_{im}\delta_{kj} + H_{mj}\delta_{ki}) \\ & + c_3(H_{ir}H_{rk}\delta_{mj} + H_{kr}H_{rj}\delta_{mi} \\ & + H_{ir}H_{rm}\delta_{kj} + H_{mr}H_{rj}\delta_{ik}) \end{aligned} \qquad (17)$$

where a_1, a_2, a_3, b_1, b_2, b_3, c_1, c_2 and c_3 are functions of the porosity of the material as well as the invariants TrH, TrH^2 and TrH^3. Tr represents "trace", e.g. $TrH = H_{11} + H_{22} + H_{33}$. However, this form is not convenient to model plane fibre networks. To reduce the plane fibre network case, the range of i, j, k, m and r in Equation 17 is reduced to 1, 2 instead of 1, 2, 3. There is another inconvenience to use of Equation 17 which is that the non-zero components of $\boldsymbol{H}$ becomes infinitely large as the fibre number density decreases. For example, using the approximation in Equation 12,

$$H_{11} = \frac{1}{2Q_0} \qquad H_{22} = \frac{1}{\pi Q_0} \qquad H_{ij} = 0 \text{ otherwise} \qquad (18)$$

for the fabric with $P = Q_0(\pi d^2/4)|\cos\theta|$. An alternative suggested by Cowin [6] is to normalize the fabric tensor H_{ij} such that $Tr\boldsymbol{H} = 1$. This removes the dependency of H_{ij} on Q_0. If $\boldsymbol{H}$ was normalized in this way for the example above, Cowin's elastic coefficient tensor for the normalized $\boldsymbol{H}$ becomes

$$C_{1111} = k_1 + k_2\Pi + k_3H_{11} + k_4H_{11}^2$$

$$\text{where } \Pi \doteq H_{11}H_{22}$$

$$C_{2222} = k_1 + k_2\Pi + k_3H_{22} + k_4H_{22}^2$$

$$C_{1122} = \frac{k_1}{3} + \frac{k_3}{6} + \frac{k_2}{6}\Pi + \frac{k_4}{6}(H_{11}^2 + H_{22}^2)$$

$$C_{1212} = C_{2121} = C_{1122} = C_{2211} = C_{1221} = C_{2112} \qquad (19)$$

For $P = Q_0(\pi d^2/4)|\cos\theta|$ the normalized fabric tensor components of the two-dimensional space are

$$H_{11} = \frac{\pi}{(\pi + 2)} \qquad H_{12} = 0 \qquad H_{22} = \frac{2}{(\pi + 2)} \qquad (20)$$

The coefficients k_2, k_3 and k_4 can then be computed by assuming that the components C_{ijkm} appearing in Equation 19 with $k_1 = 0$ be equal to the corresponding elastic coefficients of the fabric (Equation 16). This equality reduces to the solution of three simultaneous linear equations with a nonsingular matrix, and the coefficients k_2, k_3 and k_4 can be shown to be proportional to $(\pi d^2/4)Q_0D$. Hence these coefficients increase with increasing fibre density and increasing fibre stiffness as expected. The above analysis shows that the phenomenological stress–strain law proposed by Cowin is consistent with the corresponding equations of a fabric provided that the mean intercept length distribution can be represented by an ellipsoid. Although many fibre distributions can be well approximated by a mean intercept length in the form of an ellipsoids no exact (closed form) fibre distribution which gives this ellipsoidal result is known at this time.

4. Conclusions

The mechanical behaviour of short fibre composites can be described analytically in terms of even-order tensors that are expressed as functions of fibre orientation distribution [7]. For example, the stress in a fibre network can be expressed in terms of the fourth-order elasticity coefficient tensor as discussed in the previous section [5]. In some composites such as skeletal muscle or reinforced concrete the evaluation of the fibre orientation density is not difficult. But in materials with less discrete microstructure such as skin, experimental methods that would yield quantitative information on fibre (collagen) alignment have not yet been established. Mean intercept length distribution may be easier to obtain experimentally for skin using micrographs of skin taken parallel and normal to the skin surface. Equation 2 then provides an approximate method of evaluation of the number of fibres per unit normal length $(1/b^{(\alpha)})$ as a function of fibre orientation from the experimental data on mean intercept distribution. This can be accomplished by measuring L at N different angles and assume that only N distinct fibre orientations exist in the composite. Equation 2 then becomes a set of linear algebraic equations from which $(1/b^{(\alpha)})$, $\alpha = 1, 2, \ldots N$ can be computed by matrix methods.

The observation that connective tissue undergoes growth and remodelling following long durations of stretch can be described quantitatively by the use of the mean intercept length tensor M_{AB}. Let M_{AB} be the mean intercept length tensor defined by Equation 3 in the reference state described by Cartesian coordinates X_R. It can then be shown that in the absence of growth and remodelling the mean intercept length tensor in the deformed configuration (m_{ij}) is given by the following equation

$$m_{ij} = M_{AB}\frac{\partial X_A}{\partial x_i}\frac{\partial X_B}{\partial x_j} \qquad (21)$$

where x_i denotes the Cartesian coordinates of a material point in the deformed configuration. If the material remodels to preserve its original microstructural organization following expansion, m_{ij} determined by experimental data on the deformed configuration will not be equal to m_{ij} given in Equation 13 but will be identical to M_{ij} measured in the reference state. Hence the use of tensors based on fibre density or mean intercept length density distribution may be useful in the quantitative analysis of connective tissues undergoing growth and remodelling.

Appendix

Prove that a finite number N of sets of planes results in a surface $L(a_i)$ which is a continuous polyhedral surface, each side of which is plane, where L is the mean intercept in the direction of unit vector a_i.

Consider first a set of planes equally spaced at b apart with a common normal direction $\boldsymbol{n}$. The normal $\boldsymbol{n}$ may be chosen in either direction perpendicular to the planes, but after choosing it, it is held fixed. Let $\boldsymbol{a}$ be a unit vector in the direction that the mean intercept L is to be found. Choose the origin on one plane; then L' defined as the distance to the next plane (the one shown in Fig. 1) is, for the range in which $\boldsymbol{a} \cdot \boldsymbol{n} > 0$,

$$L' \boldsymbol{a} \cdot \boldsymbol{n} = b \tag{A1}$$

So

$$\frac{1}{L} = \frac{2}{b}(a_1 n_1 + a_2 n_2 + a_3 n_3) \tag{A2}$$

where we have used the fact that the crossing of each plane counts as traversing two interfaces so the mean intercept length $L = L'/2$. It follows that

$$\frac{1}{L^2} = M_{ij} a_i a_j \tag{A3}$$

where

$$M_{ij} = \frac{4}{b^2} n_i n_j \tag{A4}$$

If the terms of M_{ij} are written out in full, it is readily seen that the determinant of M_{ij} is zero, i.e.

$$|M_{ij}| = 0 \tag{A5}$$

Equation A5 follows from the fact that each row of M_{ij} is equal to the vector $[n_1, n_2, n_3]$ times a constant which varies with the row. It is also easily seen that every cofactor of the matrix is zero.

Next, consider two sets of planes and a region (i.e. a solid angle region) in which $\boldsymbol{a} \cdot \boldsymbol{n}^{(1)}$ and $\boldsymbol{a} \cdot \boldsymbol{n}^{(2)}$ are positive or zero. Here $\boldsymbol{n}^{(1)}$ and $\boldsymbol{n}^{(2)}$ are chosen normals to the sets of planes $\alpha = 1$ and $\alpha = 2$, respectively. In this discussion the directions of these normals are considered fixed once they are chosen. Because the reciprocal of mean intercept length is a measure of the number of intercepts per unit length, these reciprocals add for the two sets so

$$\frac{1}{L} = \frac{2}{b^{(1)}} a_i n_i^{(1)} + \frac{2}{b^{(2)}} a_i n_i^{(2)} \tag{A6}$$

Equation A6 may be written in the form

$$\frac{1}{L} = A_1 a_1 + A_2 a_2 + A_3 a_3 \tag{A7}$$

where

$$\begin{aligned} A_1 &= \frac{2}{b^{(1)}} n_1^{(1)} + \frac{2}{b^{(2)}} n_1^{(2)} \\ A_2 &= \frac{2}{b^{(1)}} n_2^{(1)} + \frac{2}{b^{(2)}} n_2^{(2)} \\ A_3 &= \frac{2}{b^{(1)}} n_3^{(1)} + \frac{2}{b^{(2)}} n_3^{(2)} \end{aligned} \tag{A8}$$

Comparing Equation A7 with A2, it can be seen that Equation A7 is equivalent to the mean intercept length of a single set of planes with spacing b and normal $\boldsymbol{n}$. Equating coefficients of Equations A2 and A7 gives

$$b = 2[A_1^2 + A_2^2 + A_3^2]^{-1/2} \tag{A9}$$

and

$$n_1 = \tfrac{1}{2} b A_1 \quad n_2 = \tfrac{1}{2} b A_2 \quad n_3 = \tfrac{1}{2} b A_3 \tag{A10}$$

In the derivation, one uses the fact that

$$n_1^2 + n_2^2 + n_3^2 = 1 \tag{A11}$$

which leads readily to Equation A9.

Because the expression for $(1/L)$ of the two sets of planes (Equation A7) is equal to that for the one set of planes (Equation A2), it follows that their expressions for $(1/L^2)$ are also equal. Hence the components of the tensors M_{ij} are equal for the single-plane and two-plane systems. Then as every single-plane system satisfies (Equation A5), it follows that the determinant $|M_{ij}|$ is zero for the two-plane system as well.

If there are initially three sets of planes, two can be combined into an equivalent single set of planes which in turn can be combined with the third set of planes. This reduces the three sets of planes to an equivalent single set. Hence, $|M_{ij}| = 0$ for the original set of three planes. This inductive proof can be extended to any number N of sets of parallel planes. This proves that in any region (solid angle) in which $a_i n_i^{(\alpha)}$ are all greater or equal to zero, the resulting $L(a_i)$ lie on a plane surface.

In the general case indicated by Equation 4, the choice of $\boldsymbol{n}^{(\alpha)}$ is prescribed as such that $a_i n_i^{(\alpha)}$ is greater or equal to zero. This may also be described by considering $\boldsymbol{n}^{(\alpha)}$ in a chosen fixed direction and defining $\Gamma^{(\alpha)} = \pm 1$ such that $a_i n_i^{(\alpha)} \Gamma^{(\alpha)}$ is always greater or equal to zero. Then it can be seen that $\Gamma^{(\alpha)}$ changes sign when $\boldsymbol{a}$ crosses the plane normal to $\boldsymbol{n}^{(\alpha)}$. But $L(a_i)$ is continuous at these lines because the contribution to $(1/L)$ in Equation 2 for the component α which is changing sign, is zero at the boundary. This proves that $L(a_i)$ lies on a continuous polyhedral surface for any discrete number N of sets of parallel planes. The polyhedron will be closed if at least three of the N sets of planes have normals $\boldsymbol{n}^{(\alpha)}$ which are not coplanar. If all $\boldsymbol{n}^{(\alpha)}$ are coplanar, then the surface $L(a_i)$ is a cylinder with generators perpendicular to the common plane of $\boldsymbol{n}^{(\alpha)}$. The cross-section of the cylinder is a series of straight line segments which form a continuous closed polygon with corners located along the directions $a_i \cdot n_i^\alpha = 0$.

The proofs given for N sets of parallel planes in space can be adapted to the two dimensional case of N sets of parallel fibres in a plane. It is readily seen that the description of the N sets of planes with normals all in one plane is essentially the two dimensional case when observed in the plane of the normals.

In conclusion, no finite number N sets of parallel planes in three dimensions (or N sets of parallel fibres in two dimensions) can give an ellipsoidal distribution of $L(a_i)$ in three dimensions (or elliptical distribution $L(\theta)$ in two dimensions).

References

1. W. J. WHITEHOUSE, *J. Microscopy* **101** (1974) 153.
2. T. HARRIGAN and R. W. MANN, *J. Mater. Sci.* **19** (1984) 761.
3. S. C. COWIN, *J. Biomech. Eng.* **108** (1986) 83.
4. *Idem*, in "Advances in Bioengineering", edited by N. A. Langiana (ASME Bioengineering Division, 1986) p. 26.
5. A. TÖZEREN and R. SKALAK, *J. Theoret. Biol.* **130** (1988) 337.
6. S. C. COWIN, *Mech. of Mater.* **4** (1985) 137.
7. S. G. AVANI and C. L. TUCKER III, *J. Rheol.* **31** (1987) 751.

Received 2 February
and accepted 13 June 1988